Available online at www.sciencedirect.com
SCIENCE DIRECT®
PERGAMON
International Journal of Heat and Mass Transfer 46 (2003) 3655–3660
International Journal of HEAT and MASS TRANSFER
www.elsevier.com/locate/ijhmt

Cubical-cavity natural-convection benchmark experiments: an extension

M.A.H. Mamun [a], W.H. Leong [b,*], K.G.T. Hollands [a], D.A. Johnson [a]

[a] Department of Mechanical Engineering, University of Waterloo, Waterloo, Ontario, Canada N2L 3G1
[b] Department of Mechanical, Aerospace and Industrial Engineering, Ryerson University, 350 Victoria Street, Toronto, Ontario, Canada M5B 2K3

Received 1 November 2002; received in revised form 8 March 2003

Abstract

An extension to a previously published work, this paper defines a new "diamond" orientation for the cubical-cavity benchmark problem in natural convection, and it presents new measurements on this as well as on a previously-treated orientation. Thus, measured were the average Nusselt number for an air-filled cubical cavity with two opposing isothermal faces and the remaining four sides having a linear temperature rise from the cold-face temperature to the hot-face temperature. The 95% confidence-limit uncertainties for Nusselt numbers (*Nu*) are around 1.2% for Rayleigh numbers, *Ra*, ranging from 10^4 to 3×10^8, and also for the "heating-from-the-side" orientation at $Ra = 3 \times 10^8$. Thus the results are considered suitable for the testing of computational codes.

1. Introduction

A natural convection benchmark study providing experimental data suitable for testing CFD codes was reported by Leong et al. [1,2]. They investigated natural convection in a cubical air-filled cavity with two opposing isothermal faces and the remaining four sides (called the side-walls) having a linear temperature variation from the cold face temperature to the hot face temperature. Three orientations of the cubical cavity were studied (see Fig. 1): one, called here "heating-from-the-side" had $\varphi = 90°$ and $\psi = 0°$ in Fig. 1, another, called here "heating-from-below" orientation, had $\varphi = 0°$ and $\psi = 0°$, while the third, called here the "singly-inclined" orientation, had the hot and cold faces inclined at 45° (i.e. $\varphi = 45°$ and $\psi = 0°$). Their study provided precise ($\sim \pm 1.2\%$ accuracy) measurements of the average Nusselt number, *Nu*, at the cold face for Rayleigh number, *Ra*, equal to 10^4, 4×10^4, 10^5, 10^6, 10^7 and 10^8.

This Leong et al. benchmark problem was selected as a validation exercise for the ICHMT 2nd International Symposium on Advances in Computational Heat Transfer, which took place in 2001. Here, validation attempts were made by ten sets of workers (e.g., [3–5]), and the findings of all these attempts were summarized by Pepper and Hollands [6,7]. Some of these various numerical results matched the experimental values within experimental uncertainty (particularly for the lower Rayleigh number values and at the heating-from-the-side orientation). On the other hand, not one set of worker's results suitably matched the entire set of measured *Nu* values, despite the diversity of numerical approaches. Moreover the results of the various sets of workers differed significantly from each other.

This high degree of interest and incomplete CFD confirmations indicate that work in this area still needs to be done, and they suggest that an extension providing further data is justified. Here the experimental emphasis should be on providing data for more advanced problems, suitable for attack by CFD workers once they can

* Corresponding author. Tel.: +1-416-979-5000x7706; fax: +1-416-979-5265.
E-mail address: weyleong@ryerson.ca (W.H. Leong).
URL: http://www.ryerson.ca/~weyleong/benchmark.

0017-9310/03/$ - see front matter © 2003 Elsevier Ltd. All rights reserved.
doi:10.1016/S0017-9310(03)00155-8

Nomenclature

c_p	specific heat at constant pressure of air
g	acceleration due to gravity
k	thermal conductivity of air
L	side length of cubical cavity
Nu	average Nusselt number over the cold plate, $1 + q_{conv}L/(k\Delta TL^2)$
q_{conv}	convective heat flow into the cold plate
Ra	Rayleigh number, $g\beta\Delta TL^3c_p\rho^2/(\mu k)$
T_h, T_c	temperature of hot and cold plate, respectively
T_m	mean temperature, $(T_h + T_c)/2$

Greek symbols

β	volumetric thermal expansion coefficient of air
ΔT	temperature difference, $T_h - T_c$
μ	viscosity of air
ρ	density of air
φ, ψ	angles defining the orientation of the cubical cavity, see Fig. 1

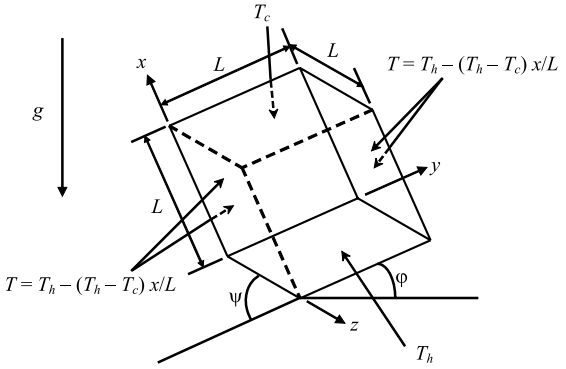

Fig. 1. Sketch defining the various orientations of the cubical cavity. The diamond orientation has $\varphi = 45°$ and $\psi = 45°$.

successfully simulate the current set of experiments. This need has provided the motivation for the present work, which extends the study of Leong et al. [1,2] by providing precise measurements of the Nusselt number for a new orientation and also some new data at higher Rayleigh number than those covered by Leong et al.

The new orientation has the cubical cavity standing on one corner with the diagonal between that lowest corner and the opposite corner aligned vertically: i.e., $\varphi = 45°$ and $\psi = 45°$ in Fig. 1. (Note that in this orientation, the hot face constitutes one of the four lower faces of the cavity.) This "doubly-inclined" orientation will, for brevity, be referred to as the "diamond" orientation. The flow in this orientation is expected to combine the Benard-like flow of the heating-from-below orientation with the boundary layer-like flow of the heating-from-the-side orientation. In this, it is similar to the singly-inclined orientation, but the combining of the two flows is expected to be more complex and subtle here. To the authors' knowledge, no previous studies are available for the diamond orientation.

The new data at higher Ra was obtained using higher temperature differences. The data is restricted to the heating-from-the-side and diamond orientations and gives Nu at $Ra = 2 \times 10^8$ and at $Ra = 3 \times 10^8$.

The above-mentioned high level of interest in a CFD validation exercise demonstrates the usefulness to CFD workers of measured Nusselt numbers *in themselves*: that is, without there being accompanying measurements of field variables—such as velocity and temperature. Perhaps this is because agreement with accurate experimental Nusselt number is a *sine qua non* of any suitable CFD code. At the same time, the present authors recognize the usefulness of field measurements for trouble-shooting codes and providing insights into the flow patterns that might be expected. For this reason, they are currently extending their experimental work to measuring the velocity field, using the particle image velocimetry (PIV) technique. Preliminary results [8] are promising.

2. Experiment

2.1. Apparatus

The experiment used the identical air-filled cubical cavity as used by Leong et al. The cavity has its two opposing isothermal plates maintained at different temperatures by circulating water through tubes soldered to their rear faces. The four adjacent side-walls are plates of highly-conducting copper to give an essentially linear temperature profile. The temperature "jumps" that would otherwise occur at the junctions between plates are removed by judicious electrical heating. In addition, the model incorporates means for measuring the heat transfer at the cold wall. The same pressure tank as had been used by Leong et al. was used here to contain the cavity; this permitted the air pressure to be varied, which provided the means for varying the Rayleigh number. New mechanical means were developed to put the cube into the diamond orientation.

2.2. Procedure

As had been done by Leong et al., eighteen independent measurements of *Nu* were made at each Rayleigh number setting, and these were averaged. The low Rayleigh number runs (those having $Ra \leqslant 10^8$) used (except as noted below) eighteen combinations of the values of the mean temperature T_m, and the temperature difference, ΔT, the same ones as were used by Leong et al. These were typically $T_m \approx 300$ K and $\Delta T \approx 7$ K, and for each combination, the air pressure was adjusted so as to give a Rayleigh number very close to the prescribed one (a correction is applied to the Nusselt number to account for the slight difference). The new high Rayleigh number runs (those having $Ra > 10^8$) used slightly higher values of T_m and decidedly higher values of ΔT: more specifically, they used values of T_m ranging from 308 to 312 K and values of ΔT ranging from 22 to 26 K. Again, the air pressure was adjusted to give the prescribed *Ra*. The remaining details of the experimental model, method, and apparatus are described by Leong et al. [1,2] and will not be repeated here.

2.3. Results

The Nusselt number results for the diamond orientation at low Rayleigh numbers are presented in Table 1, in which the 95% confidence limits of uncertainty on *Nu* are also shown. The new measurements at higher *Ra* values are similarly shown in Table 2. As has been mentioned, each tabulated Nusselt number is the average of eighteen independent measurements of the Nusselt number at that *Ra*, and the standard deviation of these eighteen measurements (as well as the bias error) was used in calculating the corresponding 95% confidence limit. The average uncertainty in *Nu* in Table 1 is 1.23%, and this is comparable to the accuracy of Leong et al.'s experiments. Similar values of the uncertainty are found in Table 2.

Table 1
Measured Nusselt number results at diamond orientation

Ra	*Nu*
1×10^4	1.676 ± 0.026
4×10^4	2.763 ± 0.033; 2.818 ± 0.033
1×10^5	3.856 ± 0.043
1×10^6	8.012 ± 0.092
1×10^7	15.77 ± 0.19
1×10^8	32.84 ± 0.39

Table 2
Results at higher Rayleigh numbers

Orientation	*Ra*	*Nu*
Heating-from-the-side	3×10^8	38.12 ± 0.45
Diamond	2×10^8	40.46 ± 0.48
Diamond	3×10^8	46.69 ± 0.55

Two different sets of Nusselt numbers were obtained at $Ra = 4 \times 10^4$: one set with *Nu* approximately equal to 2.76 and another set with *Nu* approximately equal to 2.82. Since the lower value is out of the range of uncertainty of the higher value and vice versa, the observation of two distinct sets could not be attributed to experimental error, and for this reason the two sets were averaged and kept separate, forming two different *Nu* values at this *Ra*. (It should be mentioned that Leong et al. [2] had also discovered two values of Nusselt number at a particular Rayleigh number, this time at $Ra = 10^5$ for the heating-from-below orientation.) There were a total of 21 independent measurements of *Nu* at $Ra = 4 \times 10^4$; because this is such an interesting case, three additional measurements were made for this Rayleigh numbers.

The $Nu = 2.76$ result in Table 1 is the average of eight independent measurements at $Ra = 4 \times 10^4$, and the uncertainty shown is based on this many data points; similarly the $Nu = 2.82$ result is the average of thirteen independent measurements at $Ra = 4 \times 10^4$, and the uncertainty shown is based on this many data points.

Which of the two *Nu*-values is actually observed was not found to depend on either the ΔT or the T_m used. This is in contrast to the observations of Leong et al. [2], who found that the *Nu*-value observed in any measurement correlated closely with the value of the mean temperature T_m used in that experiment.

The plot of *Nu* vs. *Ra* is presented in Fig. 2, for the entire Rayleigh number range. The relation between *Nu* and *Ra* was found to be fitted by the following equation, which has a maximum deviation of about 6.5% from the experimental data:

$$Nu = 0.09649 Ra^{0.3168} \quad (1)$$

2.4. Discussion

A comparison of the results of Leong et al. [2] and the present results in Fig. 3 shows that for *Ra* up to 10^5, the Nusselt number for the diamond orientation is greater than that for any of the other three orientations (i.e., heating-from-below, heating-from-the-side, or singly-inclined). In contrast, for $10^6 \leqslant Ra \leqslant 10^8$, the Nusselt number at the diamond orientation is smaller than that of the singly-inclined position and greater than that for either of the other two orientations. However it appears that the Nusselt number at the diamond orientation is approaching that of the singly-inclined position as *Ra* goes beyond 3×10^8, if the Nusselt numbers of both orientations keep increasing at the same trends.

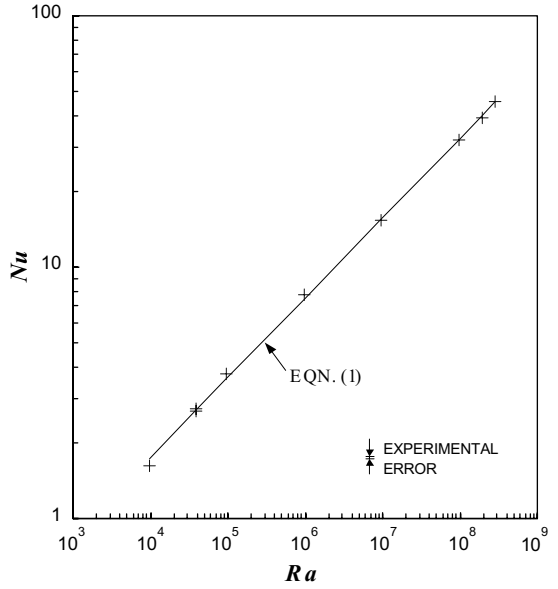

Fig. 2. Plot of *Nu* vs. *Ra* over the entire range of *Ra* in the experiments, as well as a straight line fit to the data.

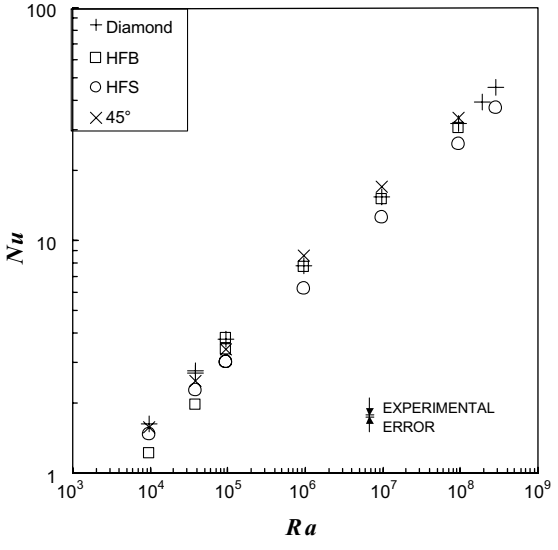

Fig. 3. Comparison of the present data with the data of Leong et al. [2]. Note: HFB, heating-from-below; HFS, heating-from-the-side; 45°, singly-inclined.

Leong et al. did CFD simulations of their low *Ra* experiments, and found that in order to get a CFD result that lay within the experimental uncertainty of the measured Nusselt number, it was necessary to use a variable-property simulation, and they recommended that future CFD workers who may wish to test their code against the benchmark experiments should use a primitive-variable, variable-property formulation, setting $T_c = 300$ K and $T_h = 307$ K, and $L = 0.1272$ m. The same recommendation is made for the diamond-orientation data reported in Table 1. To test their code against the high Rayleigh number results in Table 2, it is recommended that CFD workers use a similar primitive-variable, variable-property formulation, setting $L = 0.1272$ m, as before, but now setting $T_c = 298$ K and $T_h = 322$ K.

3. Comparison with some CFD simulations

A CFD study using TASCflow3D (a product of AEA Technology Engineering Software Ltd.) and FLUENT (a product of Fluent Inc.) was done to investigate the phenomenon at $Ra = 4 \times 10^4$ for the diamond orientation. Although it was expected that at this Rayleigh number, the flow should be laminar and steady, unsteady as well as steady simulations were attempted. TASCflow3D and FLUENT use the finite volume method to set up the three-dimensional Navier–Stokes equations and the energy equation. The temperature conditions for the simulation were as follows: $T_c = 304$ K and $T_h = 312$ K. The pressure was set to that value which will give the desired Rayleigh number of $Ra = 4 \times 10^4$, which is about 17.26 kPa. The maximum dimensionless residual for each transport equation is considered to be less than 10^{-5} for convergence.

The simulation was done both for the constant fluid property (CFP) case and for the variable fluid property (VFP) case using TASCflow3D. For the CFP simulation k, μ, β and c_p were evaluated at T_m and p and the ideal gas law was used to evaluate ρ at T_m and p. For the VFP simulation Sutherland's law was used for k and μ, the ideal gas law was used for ρ and β and a temperature dependent equation was used for c_p. The whole cavity was considered for the simulation. A rectilinear grid with a power law distribution of nodes was used in each of the three directions with fine grids close to the walls. The starting condition of the air was assumed to be stationary air at uniform temperature over the whole cavity. Three different grid sizes were used (i.e. $21 \times 21 \times 21$, $41 \times 41 \times 41$ and $81 \times 81 \times 81$ with corresponding first node spacing of 3.989, 1.110 and 0.1436 mm, respectively) and the results of the grid refinement study are shown in Table 3. The grid-independent *Nu* were also calculated using repeated Richardson extrapolation (RRE) [9] from the results and presented in the last row of Table 3. The results for the grid $81 \times 81 \times 81$ are very close to that of the RRE results. For both CFP and VFP analyses, the *Nu* for cold plate are all slightly greater than that for hot plate for all grid sizes, with a maximum difference of only 0.28% for the coarse grid $21 \times 21 \times 21$.

Table 3
Numerical results for $Ra = 4 \times 10^4$ for a grid refinement study

Grid	Variable fluid properties				Constant fluid properties			
	Nu (cold wall)	% Diff. w.r.t. fine grid	*Nu* (hot wall)	% Diff. w.r.t. fine grid	*Nu* (cold wall)	% Diff. w.r.t. fine grid	*Nu* (hot wall)	% Diff. w.r.t. fine grid
$21 \times 21 \times 21$	2.8981	5.15	2.8899	5.09	2.8839	6.03	2.8758	5. 86
$41 \times 41 \times 41$	2.7622	0.22	2.7559	0.22	2.7322	0.45	2.7259	0. 35
$81 \times 81 \times 81$	2.7562	–	2.7499	–	2.7200	–	2.7165	–
RRE	2.7559	−0.011	2.7496	−0.011	2.7189	−0.04	2.7158	−0.026

Table 4
Comparison between the numerical solutions and the experimental results

Nu (Experiment)	*Nu* (VFP)	% Diff. w.r.t experiment	*Nu* (CFP)	% Diff. w.r.t experiment
2.763 ± 0.033	2.756	−0.25	2.719	−1.59

The numerical results are close to only the experimental set at $Nu = 2.76$; and for that reason we compare the numerical results to that value. The comparisons are shown in Table 4. The *Nu* for the CFP simulation is close to experimental result but falls below the 95% confidence limits of the experimental results, differing from the experimental value by 1.59%. The *Nu* for the VFP simulation is very close to the experimental results and falls well within the 95% confidence limits of the experimental results, differing from the experimental result by only 0.25%. It is clear from the comparisons that VFP simulations are required in order to get values that are within experimental error of the experimental values. [1] This is consistent with the findings of Leong et al.

On the other hand, the phenomenon of dual *Nu* observed in the present experiments is different from the dual phenomenon observed by Leong et al. [2]. By adjusting the grid size, Leong et al. were able to achieve both of the observed Nusselt numbers, whereas in the present work it was possible to only obtain one of the observed Nusselt numbers. Also, at a given grid size, the Leong et al. simulation study found that the Nusselt number on the cold face is decidedly different from the Nusselt number on the hot face, whereas the present simulation work found no significant difference of the Nusselt numbers on the two faces. Leong et al. [2] found that which Nusselt number would be observed correlated closely to the setting of T_m; no such observation applied in the present experiments, despite the fact that the same set of temperatures was used. Simulations with different initial uniform temperature distributions—which may be equal to, lower or higher than the T_m—were attempted and they all gave Nusselt numbers close to one of the dual pair, namely $Nu = 2.76$. None came close to the other of the pair, namely $Nu = 2.82$. It appears that applying zero velocity and uniformly distributed temperature as the initial conditions (as was done here) may not be the correct assumption for the initial velocity and temperature conditions if one wants to obtain the result of $Nu = 2.82$. No further investigations were done to explore the effects of other initial velocity and temperature conditions; it was felt that such details would distract from the main purpose of this study, which was to suggest the diamond orientation as a suitable variation on the benchmark problem and to provide experimental data on it.

4. Conclusions

The natural convection Nusselt number, *Nu*, at the cold wall has been measured in an air-filled cubical cavity containing two opposing differentially heated isothermal walls and four side-walls with a linear temperature profile from the cold wall to the hot wall for the diamond orientation at the following Rayleigh number values: i.e. 10^4, 4×10^4, 10^5, 10^6, 10^7, 10^8, 2×10^8, and 3×10^8, as well as for the heating-from-the-side orientation at Rayleigh number, *Ra*, equal to 3×10^8. The 95% confidence limit uncertainties in the measured Nusselt numbers are around 1% for all Rayleigh numbers and as a consequence these results can be used for the validation of the future computational work. It is recommended that VFP models be used for CFD validation work because they provide results closest to the experimental results. The results shows that for *Ra* up to 10^5, the Nusselt number for the diamond orientation is greater than that for the heating-from-below orientation, the heating-from-the-side, or the singly-inclined orientation.

[1] Even in the VFP case the Boussinesq approximation was used to account for variation in the density. Thus differences between the CFP and the experimental results are *not* associated with the Boussinesq approximation. They must be attributable to the variability in k, μ, and c_p.

At $10^6 \leqslant Ra \leqslant 10^8$, the Nusselt number for the diamond orientation is smaller than that of singly-inclined orientation but greater than that of either the heating-from-below or heating-from-the-side orientation.

At $Ra = 4 \times 10^4$, two different experimental values of Nu were obtained at the diamond orientation: A numerical simulation study using TASCflow3D and FLUENT was done to check the phenomenon at this Rayleigh number. The numerical results are close to only one of the experimental values, with the difference from the experimental value being 0.25% when VFPs are used. The reason for getting two experimental values of Nu may possibly be due to the difference in the initial conditions. For the numerical work the initial air temperature was assumed to be uniformly distributed at a particular value and the air was at initial quiescent condition. But in the experimental work maybe these initial conditions may not have been achieved in every case.

Acknowledgements

We are indebted to Professor Pat Oosthuizen at Queen's University in Kingston, Ontario, Canada for suggesting the diamond orientation. This work was supported by a Canadian Commonwealth Scholarship to M.A.H. Mamun. Al Hodgson provided technical assistance.

References

[1] W.H. Leong, K.G.T. Hollands, A.P. Brunger, On a physically-realizable benchmark problem in internal natural convection, Int. J. Heat Mass Transfer 41 (23) (1998) 3817–3828.

[2] W.H. Leong, K.G.T. Hollands, A.P. Brunger, Experimental Nusselt numbers for a cubical-cavity benchmark problem in natural convection, Int. J. Heat Mass Transfer 42 (11) (1999) 1979–1989.

[3] K. Krepper, CHT'01: validation exercise: natural convection in an air-filled cubical cavity, in: Proceedings of the ICHMT Second International Symposium on Advances in Computational Heat Transfer, Palm Cove, Queensland, Australia, 20–25 May, 2001.

[4] J. Pallares, I. Cuesta, F.X. Grau, Natural convection in an air-filled cubical cavity contribution to the validation exercise, in: Proceedings of the ICHMT Second International Symposium on Advances in Computational Heat Transfer, Palm Cove, Queensland, Australia, 20–25 May, 2001.

[5] S. Kenjeres, S.B. Gunarjo, K. Hanjalic, Natural convection in an air-filled cubical cavity under different angles of inclination: a benchmark study, in: Proceedings of the ICHMT Second International Symposium on Advances in Computational Heat Transfer, Palm Cove, Queensland, Australia, 20–25 May, 2001.

[6] D.W. Pepper, K.G.T. Hollands, Benchmark summary of numerical studies: 3-D natural convection in air-filled enclosure, in: Proceedings of the ICHMT Second International Symposium on Advances in Computational Heat Transfer, Palm Cove, Queensland, Australia, 20–25 May, 2001.

[7] D.W. Pepper, K.G.T. Hollands, Benchmark summary of numerical studies: 3-D natural convection in air-filled enclosure, Numer. Heat Transfer Part A 42 (1/2) (2002) 1–11.

[8] M.A.H. Mamun, D.A. Johnson, K.G.T. Hollands, Natural convection heat transfer and flow measurement across a cubical cavity, in: Proceedings of the CSME Forum 2002, Queen's University, Kingston, Ontario, Canada, 21–24 May, 2002, Canadian Society for Mechanical Engineering, Ottawa.

[9] D. Zwillinger, Handbook of Integration, John Bartlett Publisher, Boston, 1992.